

# EEG Emotion Copilot: Optimizing Lightweight LLMs for Emotional EEG Interpretation with Assisted Medical Record Generation

Hongyu Chen<sup>id</sup>, Weiming Zeng<sup>id</sup>, *Senior Member, IEEE*, Chengcheng Chen<sup>id</sup>, Luhui Cai<sup>id</sup>, Fei Wang<sup>id</sup>, Yuhu Shi<sup>id</sup>, Lei Wang<sup>id</sup>, Wei Zhang<sup>id</sup>, Yueyang Li<sup>id</sup>, Hongjie Yan<sup>id</sup>, Wai Ting Siok<sup>id</sup> and Nizhuan Wang<sup>id</sup>

**Abstract**—In the fields of affective computing (AC) and brain-machine interface (BMI), the analysis of physiological and behavioral signals to discern individual emotional states has emerged as a critical research frontier. While deep learning-based approaches have made notable strides in EEG emotion recognition, particularly in feature extraction and pattern recognition, significant challenges persist in achieving end-to-end emotion computation, including real-time processing, individual adaptation, and seamless user interaction. This paper presents the EEG Emotion Copilot, a system optimizing a lightweight large language model (LLM) with 0.5B parameters operating in a local setting, which first recognizes emotional states directly from EEG signals, subsequently generates personalized diagnostic and treatment suggestions, and finally supports the automation of assisted electronic medical records. Specifically, we demonstrate the critical techniques in the novel data structure of prompt, model pruning and fine-tuning training, and deployment strategies aiming at improving real-time performance and computational efficiency. Extensive experiments show that our optimized lightweight LLM-based copilot achieves an enhanced intuitive interface for participant interaction, superior accuracy of emotion recognition and assisted electronic medical records generation, in comparison to such models with similar scale parameters or large-scale parameters such as 1.5B, 1.8B, 3B and 7B. In summary, through these efforts, the proposed copilot is expected to advance the application of AC in the medical domain, offering innovative solution to mental health monitoring. The codes will be released at [https://github.com/NZWANG/EEG\\_Emotion\\_Copilot](https://github.com/NZWANG/EEG_Emotion_Copilot).

**Index Terms**—Lightweight LLM, Model pruning, Model fine-tuning, Emotion recognition, Assisted electronic medical record

## I. INTRODUCTION

This work was supported by The Hong Kong Polytechnic University Start-up Fund [Project ID: P0053210], The Hong Kong Polytechnic University Faculty Reserve Fund [Project ID: P0053738] and the National Natural Science Foundation of China [grant number: 31870979]. (Corresponding author: Weiming Zeng, and Nizhuan Wang)

Hongyu Chen, Weiming Zeng, Chengcheng Chen, Luhui Cai, Fei Wang, Yuhu Shi, Lei Wang, Wei Zhang, Yueyang Li are with the Laboratory of Digital Image and Intelligent Computation, Shanghai Maritime University, Shanghai 201306, China (e-mail: hongyuchen676@gmail.com, zengwm86@163.com, shmtu\_ccc@163.com, clh0x123@126.com, shine\_wxf@163.com, syhustb2011@163.com, sayhiwl@163.com, zhangw99591@163.com, lyy20010615@163.com).

Hongjie Yan is with Department of Neurology, Affiliated Lianyungang Hospital of Xuzhou Medical University, Lianyungang 222002, China (email: yanhjs@gmail.com).

Wai Ting Siok and Nizhuan Wang are with Department of Chinese and Bilingual Studies, The Hong Kong Polytechnic University, Hong Kong SAR, China (e-mail: wai-ting.siok@polyu.edu.hk, wangnizhuan1120@gmail.com).

THE application of affective computing (AC) in brain-machine interfaces (BMI) is emerging as a key research frontier. Affective computing [1] seeks to identify emotional states by analyzing physiological and behavioral signals, such as electroencephalograms (EEG) [2] [3], heart rate [4], facial expressions [5], voice [6], etc. Advances in this field have expanded the possibilities for BMI technology, particularly in enhancing human-machine interaction [7], [8], and increasing its potential for practical applications in rehabilitation [9], [10] and other areas [11].

The powerful capabilities of deep neural networks (DNNs) have driven rapid advancements in AC for emotion recognition via EEG signals [12], [13], with numerous deep learning approaches proposed [14], [15]. Recently, large language models (LLMs) [16], [17] built on Transformer architecture [18] have demonstrated strong contextual understanding [19]. Models such as EEG-GPT [20] and ChatGPT-BCI [21] focus primarily on brain state identification but have yet to effectively address diverse, human-centered tasks. The integration of LLMs with EEG signals to generate personalized diagnoses, treatment plans, and assisted electronic medical records remains an urgent and complex challenge with the following limitations.

Firstly, building a suitable human-based multimodal corpus from diverse databases for LLMs is a challenging task. While public datasets like Wikitext [25] and Common Crawl [26], along with specialized datasets like SEED [27] and FACED [28], offer substantial prior knowledge, this information remains fragmented. The challenge lies in linking these datasets to create a unified data structure that facilitates language model development and enables accurate responses through appropriate prompts.

Secondly, EEG signals can be viewed as a form of long text data [29], yet the signal sequences from a single channel often exhibit significant redundancy for machine learning approaches [30], [31] [32], [33]. LLMs require a considerable number of tokens [18] to process this redundancy, resulting in unnecessary computational overhead. Additionally, many AC tasks rely on EEG data from 32, 64, or more channels, further diminishing computational efficiency and presenting challenges for real-time performance. Therefore, effective data compression is critical to optimizing lightweight LLMs for real-time applications.

Finally, lightweight LLMs are optimally run locally to safeguard participant privacy and data security. While tasks based on public LLMs, such as EEG-GPT [20], appear fea-

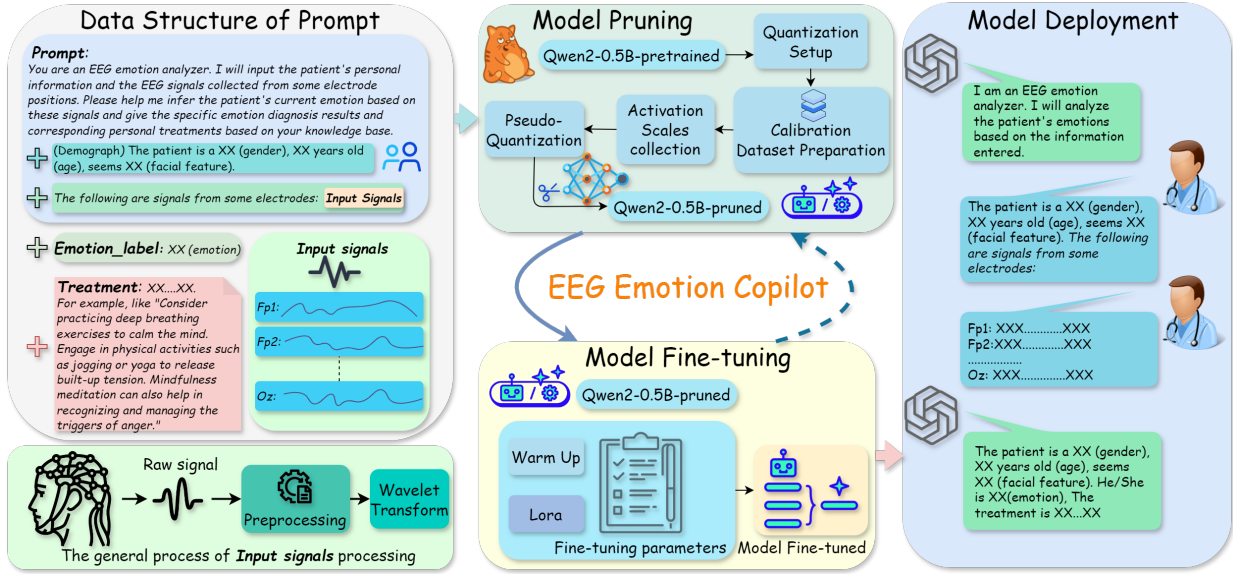


Fig. 1: Flowchart of EEG Emotion Copilot. The original EEG signal is preprocessed and transformed via wavelet to shorten the signal length. The final prompt is constructed using the initialized prompt, demographic data, emotional label, and treatment as training data. Using the Qwen2-0.5B-pretrained model [22] as an example, we prune it with the ratio of 50% and fine-tuning the pruned model directly with specific dataset. During the Model Fine-tuning stage, a warm-up phase gradually increases the learning rate, and LoRA [23] is used for fine-tuning. Finally, the model is deployed, utilizing the RAG (Retriever-Reader-Generator) technique [24] to enhance retrieval performance, and a dialogue deployment of the graphical interface to improve interactivity.

sible, many industry models necessitate powerful machines. For specific local tasks, complex DNNs are often excessively redundant. Therefore, effective model pruning is essential to achieve a lightweight language model suitable for local execution.

Therefore, we propose EEG Emotion Copilot, an intelligent system based on a lightweight, locally-running language model that utilizes EEG signals to first perform emotion recognition, subsequently generate corresponding diagnosis and treatment plans, and finally create assisted electronic medical records, as illustrated in Fig. 1.

## II. RELATED WORK

### A. Lengthy EEG Signal Embedded in Prompt

For specific tasks in LLM prompt engineering, tailored prompts are essential to obtain reasonable answers [34]. Although datasets like Wikitext [25] and Common Crawl [26] contain extensive knowledge, constructing specific datasets is necessary for optimal performance in particular tasks. In most studies on AC, researchers focus on distinguishing emotions using convolutional neural networks (CNNs) or recurrent neural networks (RNNs) [35], with EEG signals primarily used to assess model quality [36], [37]. Recently, LLMs should split EEG sequences into tokens for processing, with computational and memory requirements increasing exponentially with input length [38]. This poses challenges for LLMs deployment, especially on low-resource devices or in real-time scenarios. Although data chunking strategies [39] can split long sequences for training and deployment, the EEG data

length significantly impacts reasoning effectiveness [40], [41]. Therefore, a reasonable data compression method is necessary to LLMs.

### B. Model Pruning in Deep Learning

The Frankle and Carbin's lottery ticket hypothesis [42] posits that small subnetworks, when trained from scratch, can achieve comparable performance. Based on it, model pruning [43] has been widely applied in DNNs to reduce computational complexity and mitigate model hallucinations [44]. For instance, Li et al. [45] and Han et al. [46] introduced filter and weight pruning techniques, while Michel et al. [47] explored attention head pruning in Transformer models. Zhuang et al. [48] employed gradient-based structured pruning, and Liu et al. [49] proposed MetaPrune, which combines pruning with neural architecture search (NAS). Guo et al. [50] focused on channel pruning for efficient inference. Comprehensive surveys by Blalock et al. [51] and He et al. [52] have highlighted the effectiveness of various pruning techniques and outlined future research directions. In the context of LLMs, methods such as SparseGPT [53] and LLM-Pruner [54], primarily based on the LLaMA model [55], have demonstrated promising results on public datasets and claim faster performance on local machines. However, the hardware used for inference, such as RTX 4090 GPUs, significantly outperforms standard PCs, leaving the inference cost still relatively high. Thus, for local computations with limited resources, there remains a need for more efficient and feasible pruning methods to further reduce computational costs.

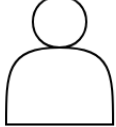
	Name: XXX Gender: XX	
	Data of Birth: XXX	
	Contact: XX Insurance: XX	
<b>Medical History</b>	<b>Physical Examination Records</b>	
Past Medical History	symptom1: ..... symptomN	
Family History		
Allergy History		
Medication History		
<b>Diagnosis Information</b>	<b>Treatment Plan</b>	
Diagnosis : XXX...XX XXX...XX  XXX...XX XXX...XX ..... XXX...XX XXX...XX	Medication Prescriptions	
	Surgical Records	
	Other Treatment Options	
<b>Laboratory Results</b>	<b>Follow-up Records</b>	
<b>Comprehensive Results</b>		
<b>Medical Expenses</b>		

Fig. 2: Schematic diagram of the assisted electronic medical record generated by intelligent copilot. It can include Basic Information, Medical History, Physical Examination Records, Diagnosis Information, Treatment Plan, Laboratory Results, Follow-up Records, and Medical Expenses.

### C. Assisted Electronic Medical Records

Electronic medical records (EMRs) date back to the 1960s [56]. With advancements in computer science and artificial intelligence (AI), EMRs have evolved from merely storing and managing patient information to incorporating more complex functionalities. Currently AI models are increasingly integrated into diagnosing mental illnesses and detecting internal organ pathologies, enhancing the capabilities of assisted EMRs. The sample of "assisted electronic medical record" is shown in Fig. 2, where the intelligent copilot can process the multimodal diagnostic data and produce accurate results. In this study, we developed a new EEG Emotion Copilot that leverages a lightweight local LLM to perform emotion recognition based on EEG signals, and to further generate the corresponding assisted EMR.

## III. METHOD

### A. Data Structures of Prompt in EEG Emotion Copilot

Fine-tuned LLMs often achieve strong performance to generate end-to-end outputs, particularly for simple classification tasks. For instance, distinguishing whether a subject's emotional state is positive or negative based on EEG data is relatively straightforward. However, distinguishing more nuanced emotions, such as nine-class emotions in FACED

dataset [28], or accurately identifying emotions in real-world scenarios, remains challenging.

For Wikitext or similar datasets, these datasets often consist of declarative sentences (left part of Fig. 3), but for tasks like logical reasoning, data are stored as question-answer pairs, as shown in the middle part of Fig. 3. Despite these advancements, current data structures encounter significant limitations when applied to EEG-based emotion diagnosis and treatment planning. These challenges arise particularly in integrating multimodal data and addressing task-specific requirements. To address these gaps, we propose a novel structure leveraging a question-answer system tailored to EEG-related tasks.

In the data structure of the proposed EEG Emotion Copilot, we initialize the system with the prompt showed in the right part of Fig. 3: "You are an EEG emotion analyzer. I will input the patient's personal information and EEG signals from specific electrode positions. Please infer the patient's current emotional state and provide a detailed diagnosis along with personalized treatments based on your knowledge base." Following initialization, we input the subject's demographic data, including gender, age, and facial features, to assess their emotional state. Next, the acquired EEG signals are processed. As illustrated in Fig. 1, preprocessing steps such as artifact removal and re-referencing are applied to the signals, followed by wavelet transformation for signal compression. These processed signals are then used as input. Finally, the structure is completed by adding emotion labels and corresponding treatment plans in the second and third sections, respectively.

### B. Model Pruning in EEG Emotion Copilot

In this study, for the flexibility and versatility, we applied the torch pruning [57] to perform the model pruning task with the pruning\_ratio equal to 0.5, and the detailed process is showed in Fig. 4.

Firstly, based on the architecture of the Qwen2-0.5B model, the total number of layers  $L$  is determined as follows:

$$\mathcal{L} = \text{Num}(\text{Qwen2\_layer}) = \text{Num}(\text{Embedding\_layer}) + \text{Num}(\text{Qwen2Decoder\_layer}) + \text{Num}(\text{Lm\_head}) = 25. \quad (1)$$

The input and output of each layer are represented as  $f_i^-$  and  $f_j^+$ , respectively, where  $0 \leq i \leq 25, 0 \leq j \leq 25$  and  $i, j \in \mathbb{N}^+$ .

Next, we construct a layer dependency graph  $\mathcal{F}$  according to [57]. Based on the symmetric mechanism of input  $f_i^-$  and output  $f_j^+$ , the dependency graph  $\mathcal{F}$  is defined as a  $2\mathcal{L} \times 2\mathcal{L}$  symmetric matrix, specifically as follows:

$$\mathcal{F}(f_i^-, f_j^+) = \mathcal{F}(f_j^+, f_i^-) = \begin{cases} 1, & \text{if } f_i^- \leftrightarrow f_j^+ \text{ or} \\ & (i = j \text{ and } \text{sch}(f_i^-) = \text{sch}(f_j^+)), \\ 0, & \text{otherwise} \end{cases}, \quad (2)$$

where  $\text{sch}(p)$  operation is used to determine which parameters in the parameter group  $p$  need to be retained. Formula 2 returns a boolean value, where  $\text{sch}(f_i^+) = \text{sch}(f_j^-)$  indicates that the two parameter groups are subject to the same pruning scheme.

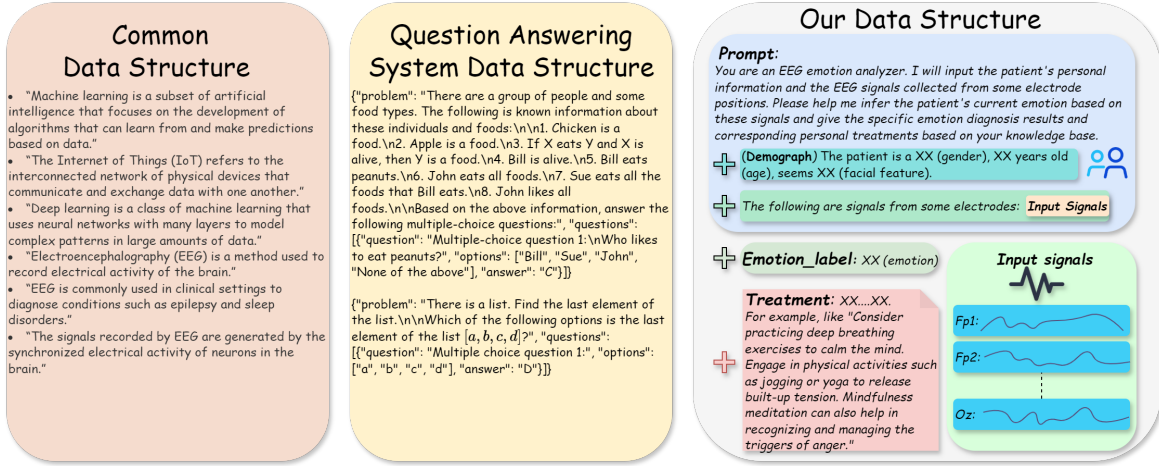


Fig. 3: Comparison of three data structures as to prompt in LLMs: the general data structure (left), the question-answering system data structure (middle), and the data structure used in the proposed EEG Emotion Copilot (right).

In addition, we use the  $\mathcal{L}_2$  norm to calculate the importance of the parameter group corresponding to each layer [57]. Based on the Qwen2 architecture, we calculate the importance  $\mathcal{I}$  of the Embedding layer, Self-Attention layer, MLP layer, and Linear layer in turn as follows:

$$\mathcal{I}(\text{embed\_tokens}) = \sum_{w \in \text{embed\_tokens}} \|w\|_2^2, \quad (3)$$

$$\mathcal{I}(s_i) = \sum_{w \in s_i} \|w\|_2^2, \quad S = \{s_i\} = \{q_{\text{proj}}, k_{\text{proj}}, v_{\text{proj}}, o_{\text{proj}}\}, \quad (4)$$

$$\mathcal{I}(m_i) = \sum_{w \in m_i} \|w\|_2^2, \quad M = \{m_i\} = \{gate_{\text{proj}}, up_{\text{proj}}, down_{\text{proj}}\}, \quad (5)$$

$$\mathcal{I}(\text{lm\_head}) = \sum_{w \in \text{lm\_head}} \|w\|_2^2. \quad (6)$$

Based on the above formula, we first group the parameters  $\mathcal{P}$  to get set  $\mathcal{P}'$ , as shown in Algorithm 1. Then, we proceed to prune the model, as shown in Algorithm 2.

#### Algorithm 1 Parameter Grouping

- 1: **Input:** Dependency graph  $\mathcal{F}$ , parameter group set  $\mathcal{P}$
- 2: **Output:** Group set  $\mathcal{P}'$
- 3: Initialize  $\mathcal{P}' \leftarrow \emptyset$
- 4: **for all**  $i \in \mathcal{L}$  **do**
- 5:     Create new group  $p \leftarrow \{k\}$
- 6:     Expand group  $p$ :
- 7:     **while** there exists an unvisited node  $j$  such that  $\mathcal{F}(f_i^-, f_j^+) = 1$  **do**
- 8:          $p \leftarrow p \cup \{j\}$
- 9:         Mark  $j$  as visited
- 10:     **end while**
- 11:      $\mathcal{P}' \leftarrow \mathcal{P}' \cup p$
- 12: **end for**
- 13: **return**  $\mathcal{P}'$

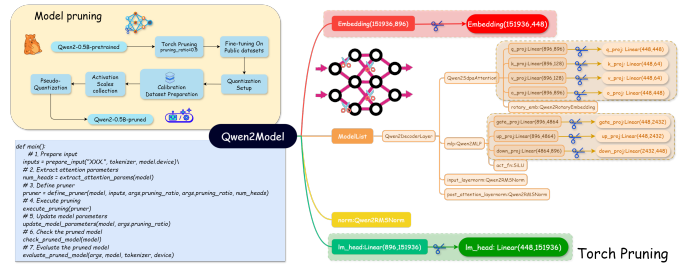


Fig. 4: Flowchart of model pruning in EEG Emotion Copilot: The upper left presents a rough framework diagram, while the right side illustrates torch pruning with a 0.5 pruning ratio. In this process, the input\_feature and out\_feature of Qwen2SdpaAttention and Qwen2MLP are halved compared to the original model. The final output of lm\_head remains unchanged, as it is directly tied to the vocabulary size. The lower left depicts a simplified torch pruning process.

#### C. Model Fine-tuning in EEG Emotion Copilot

To restore the performance of the pruned model  $\mathcal{M}'$ , we explored two fine-tuning strategies after applying torch-pruning [57], as illustrated in Fig. 5. Strategy 1 is only training the pruned model on the specific EEG dataset to focus the model on task-relevant features with Low-Rank Adaptation (LoRA) [23]. Strategy 2 firstly involves full fine-tuning the pruned model on public datasets Wikitext [25] and Common Crawl [26], to leverage their diverse categories to establish generalized features, and subsequently fine-tuning on the specific EEG dataset with LoRA. Moreover, a warm-up strategy is applied at the beginning of training to facilitate convergence and improve overall model performance.

Specifically, the model's fine-tuning process on the specific EEG dataset is illustrated in Fig. 6, dividing the training process into five steps, each with three epochs. In steps 1–4, we used 250 Hz data from 55 subjects of FACED [28]. Interestingly, the model's performance in step 3 surpassed

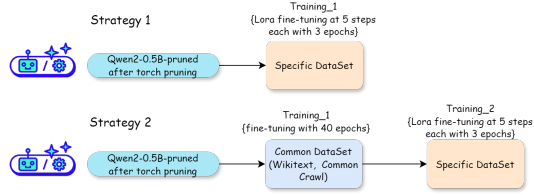


Fig. 5: Two fine-tuning strategies. Strategy 1 involves initially training the model on a specific EEG dataset tailored to the current task. Strategy 2 begins with training the model on public datasets, and subsequently fine-tuning it on a specific EEG dataset.

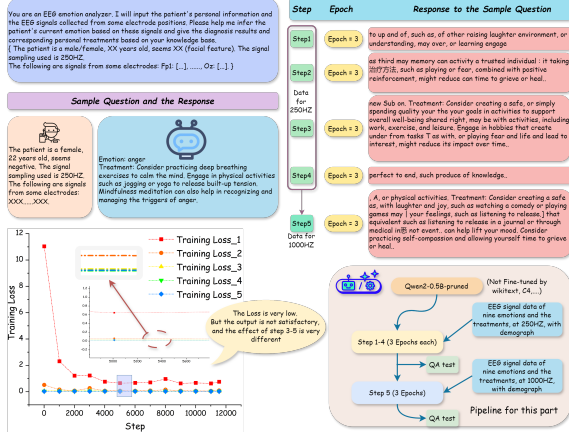


Fig. 6: Model's fine-tuning process on the specific EEG dataset. This fine-tuning process is divided into five steps, each consisting of three epochs. The first four steps utilize 250 Hz data from 55 subjects. Comparing the model's answers in steps 3 and 4 reveals that the answer in step 3 is richer in content, with no significant difference in training loss between the two steps. This suggests that overtraining lightweight models may be redundant or even detrimental. In step 5, 1000 Hz data from 68 subjects is used for training, employing the pre-trained model from step 4.

that in step 4, despite minimal differences in training\_loss, suggesting that excessive training may be unnecessary and even detrimental for lightweight models. In step 5, 1000 Hz data from 68 FACED subjects pre-trained on step 4 yielded richer responses, confirming the model's capability to learn the data structure and generate task-specific answers effectively.

#### D. Model Deployment in EEG Emotion Copilot

Given the various model deployment tools, such as `llama.cpp`, which can quantify the model based on the specific scenario and convert it into gguf format, it can be directly utilized through `ollama`, `llmstudio`, `gradio` or other tools. This process with `gradio` ultimately results in the model deployment part illustrated in Fig. 1.

#### E. Generation of Assisted Electronic Medical Records

Due to the fact that the proposed copilot involves various tasks such as emotion recognition, diagnosis, and treatment

#### Algorithm 2 Pruning Process

- 1: **Input:** Initial model  $\mathcal{M}$ , Parameter group set  $\mathcal{P}'$ , importance function  $\mathcal{I}$ , contraction strength  $\alpha$
- 2: **Output:** Pruned model  $\mathcal{M}'$
- 3: Calculate group importance:
- 4: **for all**  $p' \in \mathcal{P}'$  **do**
- 5:      $\mathcal{I}(p') \leftarrow \sum_{w \in \mathcal{P}'} \|w\|_2^2$  (See Formula 3, 4, 5, 6)
- 6: **end for**
- 7:      $\mathcal{P}'' \leftarrow \text{sort}(\mathcal{P}', \text{by } \mathcal{I})$
- 8: Select groups for pruning based on importance:
- 9: **for all**  $p'' \in \mathcal{P}''$  **do**
- 10:     **if**  $\mathcal{I}(p'') \leq \theta$  **is satisfied then**  $\# \theta$  is the threshold
- 11:          $\mathcal{P}'' \leftarrow \mathcal{P}'' \setminus p''$
- 12:     **end if**
- 13: **end for**
- 14: **return**  $\mathcal{M}'$

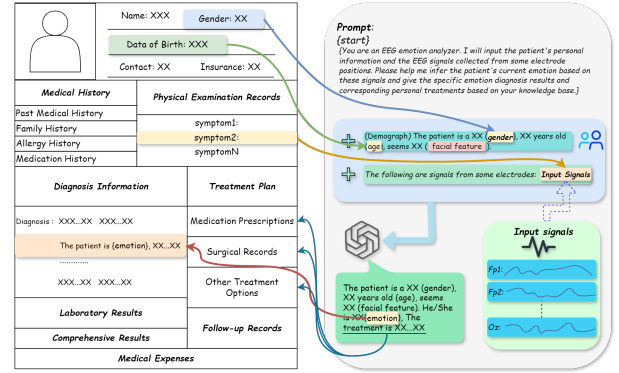


Fig. 7: Flowchart of assisted electronic medical record generation implemented in EEG Emotion Copilot.

plan design, it is sufficient to embed demographic data from different cases under various emotional states, along with the corresponding compressed EEG signals, into the training data. In downstream applications, participant data can be input into the fine-tuned model in a specific format to obtain diagnostic information and treatment plans, as shown in Fig. 7.

## IV. EXPERIMENTS

### A. Implementation Details

**Dataset:** We utilize the FACED dataset [29] to validate our copilot. This dataset includes recordings from 123 subjects, each with 32 EEG channels, as they watched 28 video clips, each lasting 30 seconds. These clips encompass nine emotions: anger, disgust, fear, sadness, neutral, amusement, Inspiration, Joy, and Tenderness. Each positive and negative emotion is represented by three clips, while the neutral emotion is depicted in four clips.

**Training Details:** In the model pruning phase, we set the pruning ratio to 0.5 and then trained on the public datasets with a learning rate of  $1e-5$ , incorporating L1 and L2 regularization terms. The training was conducted for 40 Epochs. During the LoRA fine-tuning phase, we maintained a learning rate of  $1e-5$ , applied weight decay and gradient decay, and set  $\text{LoRA}_r$  to 8,

Prompt: You are an EEG emotion analyzer. I will input the patient's personal information and the EEG signals collected from some electrode positions. Please help me infer the patient's current emotion based on this signal. The patient is a female, 22 years old, seems negative. The signal sampling used is 250Hz. The following are signals from some electrodes:  
Fp1: [...], O2: [...]

Question	Text Representation Technique	Compression method (W:Wavelet Transform $\approx$ split)	Answer	Euclidean distance	Cosine similarity
Emotion: sadness. Treatment: Try talking to a trusted friend or therapist to express and process your feelings. Engaging in activities that you once enjoyed, even if they feel difficult, can help lift your mood. Consider practicing self-compassion and allowing yourself time to grieve or heal.	Bag of Words	7500 <sup>W</sup> $\rightarrow$ 500 <sup>S</sup> $\rightarrow$ 10 <sup>W</sup> $\rightarrow$ 50	Ans1	8.246	0.348
		7500 <sup>W</sup> $\rightarrow$ 50	Ans2	8.544	0.346
Emotion: anger. Treatment: It appears to be dealing with something that triggers us, causing us tension or conflict in our life. Engaging in activities that allow us to express and process our feelings, perhaps through talking to a trusted friend or instructor, helps resolve tensions.	Word Embeddings	7500 <sup>W</sup> $\rightarrow$ 500 <sup>S</sup> $\rightarrow$ 10 <sup>W</sup> $\rightarrow$ 50	Ans1	7.011	0.900
		7500 <sup>W</sup> $\rightarrow$ 50	Ans2	6.982	0.899
Baseline		7500	Net work	\	\

Fig. 8: Two demos of paired question and answer with EEG signal lengths of 500 time points derived from compression method 1 (W $\rightarrow$ S)) and 50 time points derived from compression method 2 (W). The doctor first asks a question to the trained model based on W $\rightarrow$ S or W. For W $\rightarrow$ S, the wavelet transform initially compresses the original signal of each channel into 500 points, then divides the compressed channel signal into 10 segments. These ten sequential group data serve as training data for W $\rightarrow$ S. For W, the wavelet transform compresses the original signal of each channel into 50 points as training data. Ans1 and Ans2 are the answers from W $\rightarrow$ S and W, respectively, while the baseline represents the real answer to the question.

LoRA <sub>$\alpha$</sub>  to 32, and LoRA<sub>dropout</sub> to 0.5. The fine-tuning process spanned 15 epochs, dividing into 5 steps. Model pruning was executed on a NVIDIA A800 80G, while the fine-tuning were completed on NVIDIA GeForce RTX 4090 GPUs.

### B. Performance Validation of Varied EEG Signal Length

Regarding the effect of the compressed signal length, we first extracted the EEG signal in the FACED data and the corresponding demography according to the Data Structure in Fig. 1. We implemented two compression methods and an original control group. The question-answering process and the corresponding results are shown in Fig. 8. Although the euclidean distance and cosine similarity of Ans1 and Ans2 are similar to the baseline for the same question, Ans2 is more consistent with the baseline than Ans1, as Ans1 differs from the baseline in terms of emotion recognition. Therefore, with limited resources, it is often more effective to compress the signal to a fixed length using wavelet transforms rather than a segmented approach.

### C. Performance Comparison with Lightweight Models

To better validate our experimental hypothesis, we combine the strategies outlined in Fig. 6 and Fig. 8. First, we divide the training process based on the data derived from compression method 1, into five steps, with each step trained for 3 epochs. For each step's checkpoint (i.e., checkpoint1-n), we perform classification of content generation for the nine emotions described in III-A, followed by classification for three emotions (positive, negative, neutral). For comparison, we use Qwen2-0.5B as the base model, training it for 6 epochs under identical experimental conditions to obtain base\_model-1, and perform classification, as shown in Table I.

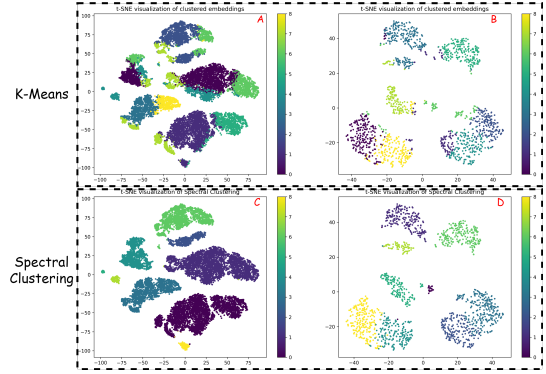


Fig. 9: t-SNE [61] visualization of K-Means (A-B) and spectral clustering (C-D) results of embeddings based on the EEG signal length=500 (compression method 1) and EEG signal length=50 (compression method 2) in Fig. 8, respectively.

Next, we fine-tuned the models based on the data derived from compression method 2. Specifically, we fine-tuned the pruned model in three steps, with 3, 3, and 3 epochs respectively, and perform classification for both the nine emotions and the three emotions. For consistency, Qwen2-0.5B is also trained for 6 epochs to obtain base\_model-2, after which the corresponding classification experiment is conducted, as shown in Table I.

Additionally, we include opt-350m [58], LiteLlama, and gpt-sw3-356m as baseline references. Indeed, the checkpoint1-n model of Model 1 did not achieve ideal results on both tasks compared to the base\_model-1. However, considering the F1 scores across multiple epochs of training, the model's performance on this task gradually improved. In Model 2, the performance of checkpoint2-2 and checkpoint2-3 showed significant improvement compared to models with the similar parameter size, and they also consumed less average response time.

### D. Performance Comparison with Heavyweight Models

In Table II, we present the results of emotion recognition for Qwen2-1.5B [22], InternLM2.5-1.8B [59], Qwen2.5-3B [60], and Qwen2.5-7B [60], and InternLM2.5-7B [59]. Surprisingly, the results were not as impressive as expected. The reason for this is that the default setting for top-k is 50. But even if top-k is set to 1, the results are still not ideal. For the heavyweight models, their responses are more flexible due to their larger knowledge storage, allowing them to generate a wider range of answers. This also indicates that, despite the very low loss during training, which might suggest model fitting, the actual responses in specific scenarios are dissatisfactory.

Furthermore, we first use the pre-trained all-MiniLM-L6-v2 model for text representation. Specifically, we combine the "prompt" and "treatment" from each record into a single string and generate the corresponding embedding vectors. These embeddings are then subjected to K-Means clustering and spectral clustering [62] for unsupervised learning, with the number of clusters set to 9. The t-SNE [61] is applied to reduce the dimensionality of the embedding and visualize the results, as shown in Fig. 9.

TABLE I: Performance Comparison Of Competing Light-Weight Models

Compression Method	Model	Parameters	Storage_size	Precision	Epoch	Nine Emotion Recognition		Three Emotion Recognition		
						F1	Avg. RT (s)	F1	Avg. RT (s)	
W→S	Our Model 1									
	checkpoint1-1	0.15B	0.294G	bf16	3	0.080	<u>0.430</u>	0.216	<u>0.420</u>	
	checkpoint1-2	0.15B	0.294G	bf16	3	0.096	0.510	0.324	0.510	
	checkpoint1-3	0.15B	0.294G	bf16	3	0.100	0.540	<b>0.376</b>	0.540	
	checkpoint1-4	0.15B	0.294G	bf16	3	0.093	0.600	0.359	0.610	
	checkpoint1-5	0.15B	0.294G	bf16	3	<b>0.103</b>	0.610	0.340	0.580	
	base_model-1 [22]	0.50B	0.920G	bf16	6	<b>0.143</b>	<u>1.120</u>	<b>0.445</b>	1.220	
	opt-350m-1 [58]	0.35B	0.647G	bf16	15	0.036	3.240	0.037	3.180	
	LiteLlama	0.46B	0.901G	bf16	15	0.041	1.910	0.057	1.900	
	gpt-sw3-356m	0.47B	1.580G	bf16	15	0.035	1.160	0.035	<u>1.180</u>	
W	Our Model 2									
	checkpoint2-1	0.15B	0.294G	bf16	3	0.118	0.580	0.432	0.590	
	checkpoint2-2	0.15B	0.294G	bf16	3	<b>0.346</b>	0.590	<b>0.980</b>	0.590	
	checkpoint2-3	0.15B	0.294G	bf16	3	0.339	<u>0.550</u>	0.960	<u>0.540</u>	
	base_model-2 [22]	0.50B	0.920G	bf16	6	<b>0.153</b>	1.230	<b>0.450</b>	1.290	
	opt-350m [58]	0.35B	0.647G	bf16	15	0.037	3.960	0.038	4.090	
	LiteLlama	0.46B	0.901G	bf16	15	0.036	2.120	0.036	2.120	
	gpt-sw3-356m	0.47B	1.580G	bf16	15	0.036	<u>1.070</u>	0.036	<u>1.260</u>	

Note: W→S and W denote the compression method described in Fig. 8, respectively. checkpoint1-n ( $n \in \{1,2,3,4,5\}$ ) denotes the model trained in different training step of Model 1, checkpoint2-n' ( $n' \in \{1,2,3\}$ ) denotes the model trained in different training step of Model 2.

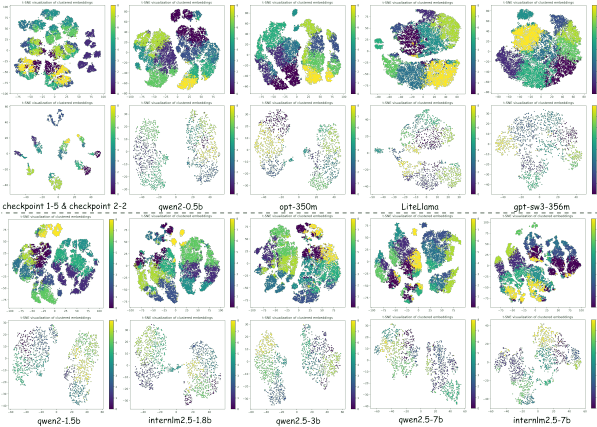


Fig. 10: Clustering results of data for compression method 1 and 2 described in Fig. 8 using various models mentioned in Table I and II with K-Means clustering and t-SNE [61] visualization of the text embeddings.

In addition, we investigate the clustering performance for data of compression method 1 and 2 respectively in Fig. 8 by applying the same procedure to a range of models included in Table I and II. We convert the text into the appropriate input format using the tokenizer, extract the hidden states from the final layer, and apply average pooling to generate fixed-length text embedding vectors. These embeddings are clustered using K-Means, and dimensionality reduction is performed using the t-SNE for visualization, as shown in Fig. 10. Indeed, as illustrated in Fig. 9 and 10, the visualization suggests that corpora of two different lengths are not easily clustered. Specifically, compared to the data of Model 1, the data of Model 2 exhibits a higher degree of aggregation, which directly corresponds to a reduction in computational load.

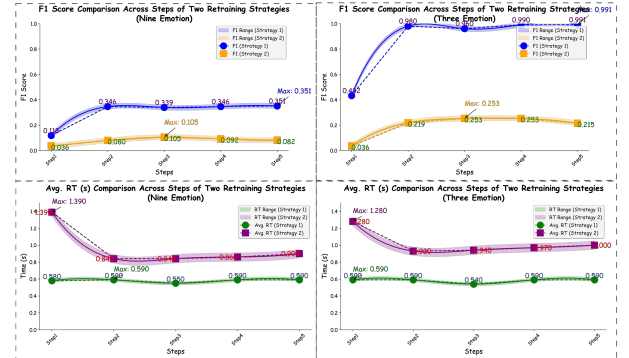


Fig. 11: Performance comparison as to F1 and Avg. RT of nine and three emotion classification across steps of two fine-tuning strategies.

### E. Model Fine-tuning Strategy Comparison After Pruning

To evaluate the two fine-tuning strategies outlined in Fig. 5, we adopted compression method 2 show in Fig. 8 for comparison. According to the results from Table I and Fig. 11, we found that Strategy 1 demonstrated better performance in Table I than Strategy 2 did in the lightweight models fine-tuning process.

### F. Assisted Electronic Medical Record Generation with Our Copilot

Fig. 12 illustrates an example of using our EEG Emotion Copilot to create an electronic medical record. Initially, the starting sentence of the prompt is provided, followed by the addition of demographic information of the subjects, including age, gender, and certain facial features. Finally, the pre-processed and compressed signal is incorporated to complete the prompt, which is then input into EEG Emotion Copilot. The

TABLE II: Performance comparison Of Heavy-Weight Models

Compression Method	Model	Parameters	Storage Size	Precision	Epoch	Nine Emotion Recognition		Three Emotion Recognition	
						F1 (Top-K=50)	Avg. RT (s)	F1 (Top-K=50)	Avg. RT (s)
W→S	qwen2-1.5b-1 [22]	1.5B	3.091G	bf16	3	0.095	2.950	<b>0.314</b>	2.900
	Internlm2.5-1.8b-1 [59]	1.8B	3.780G	bf16	3	0.036	5.870	0.035	5.910
	qwen2.5-3b-1 [60]	3B	6.170G	bf16	3	<b>0.111</b>	4.260	0.041	10.960
	qwen2.5-7b-1 [60]	7B	15.230G	bf16	2	0.051	<u>1.410</u>	0.152	<u>2.100</u>
	Internlm2.5-7b-1 [59]	7B	14.200G	bf16	2	0.082	10.090	0.039	10.090
W	qwen2-1.5b-2 [22]	1.5B	3.091G	bf16	3	0.074	3.730	<b>0.328</b>	3.510
	Internlm2.5-1.8b-2 [59]	1.8B	3.780G	bf16	3	0.036	6.320	0.041	4.470
	qwen2.5-3b-2 [60]	3B	6.170G	bf16	3	<b>0.133</b>	3.680	0.114	3.760
	qwen2.5-7b-2 [60]	7B	15.230G	bf16	2	0.036	<u>0.020</u>	0.038	<u>0.240</u>
	Internlm2.5-7b-2 [59]	7B	14.200G	bf16	2	0.082	10.260	0.042	7.300
Compression Method	Model	Parameters	Storage Size	Precision	Epoch	Nine Emotion Recognition		Three Emotion Recognition	
						F1 (Top-K=1)	Avg. RT (s)	F1 (Top-K=1)	Avg. RT (s)
W→S	qwen2-1.5b-1 [22]	1.5B	3.091G	bf16	3	<b>0.095</b>	1.880	0.318	2.590
	Internlm2.5-1.8b-1 [59]	1.8B	3.780G	bf16	3	0.036	7.100	0.036	5.830
	qwen2.5-3b-1 [60]	3B	6.170G	bf16	3	0.080	3.810	<b>0.342</b>	4.500
	qwen2.5-7b-1 [60]	7B	15.230G	bf16	2	0.040	<u>0.690</u>	0.036	<u>0.870</u>
	Internlm2.5-7b-1 [59]	7B	14.200G	bf16	2	0.090	8.950	0.040	9.390
W	qwen2-1.5b-2 [22]	1.5B	3.091G	bf16	3	0.081	3.780	<b>0.292</b>	4.170
	Internlm2.5-1.8b-2 [59]	1.8B	3.780G	bf16	3	0.036	7.210	0.036	4.470
	qwen2.5-3b-2 [60]	3B	6.170G	bf16	3	0.036	6.320	0.038	4.470
	qwen2.5-7b-2 [60]	7B	15.230G	bf16	2	0.051	4.870	0.110	4.920
	Internlm2.5-7b-2 [59]	7B	14.200G	bf16	2	0.081	11.640	0.041	9.790

EEG Emotion Copilot first analyzes the data to generate an answer, which is subsequently transformed into the record through format conversion.

## V. DISCUSSION

### A. Data Structure of Prompt

We developed a comprehensive human-based dataset that integrates both public knowledge datasets and specialized emotion datasets, facilitating the construction of a robust data structure to drive the development of LLMs. By employing effective prompting strategies, we enhanced the model’s ability to generate contextually relevant responses. Furthermore, while the performance of the models may not be exceptionally high, as illustrated in Table I and II, language remains more challenging to cluster unsupervised compared to other data types [63]. Nonetheless, by utilizing a pretrained sentence transformer model of an appropriate size, the model is still able to capture the underlying emotional features of the language to some extent as demonstrated in the spectral clustering shown in Fig. 9, despite potential issues with feature imbalance.

### B. Data Redundancy in EEG Signal Processing

We addressed the issue of data redundancy inherent in EEG signal processing. Through efficient data compression techniques, we optimized the handling of long sequences of EEG data, significantly improving computational efficiency and facilitating real-time emotion computation. However, simply compressing signal data is computationally intensive in many cases, and in complex scenarios, more channel signals are needed. Therefore, if LLMs can generate dense channel signals using only a few channel data and then analyze the emotions of the subjects [64], [65], computational efficiency will be greatly improved.

### C. Patient Privacy and Model Efficiency

We emphasized the importance of patient privacy by ensuring that our model can run locally. We explored model pruning strategies to create a lightweight version of the language model, making it feasible to deploy in environments with limited computational resources while maintaining performance.

### D. Performance of Lightweight Models

We performed model pruning and compared the performance of the models obtained through the two fine-tuning methods illustrated in Fig. 5. It was found that the results obtained using Strategy 1 for fine-tuning were superior. Furthermore, as shown in Table I and II, the lightweight pruned model achieved through multi-step fine-tuning demonstrated better performance compared to other models with larger parameter sizes.

### E. Hallucination of Heavyweight Models

While a low training loss suggests a good fit to the training data, it does not necessarily reflect the model’s true performance, as the generated responses may still fail to meet expectations or even diverge significantly [66]. This issue is particularly evident in 7B and larger models, where the hallucination problem becomes more pronounced in specialized domains. These findings also suggest that lightweight models may be better suited for such domain-specific generation tasks.

## VI. CONCLUSION

In this paper, we present EEG Emotion Copilot, a lightweight and locally-running LLM designed for emotional recognition using EEG signals and the generation of corresponding treatment plans for assisted electronic medical

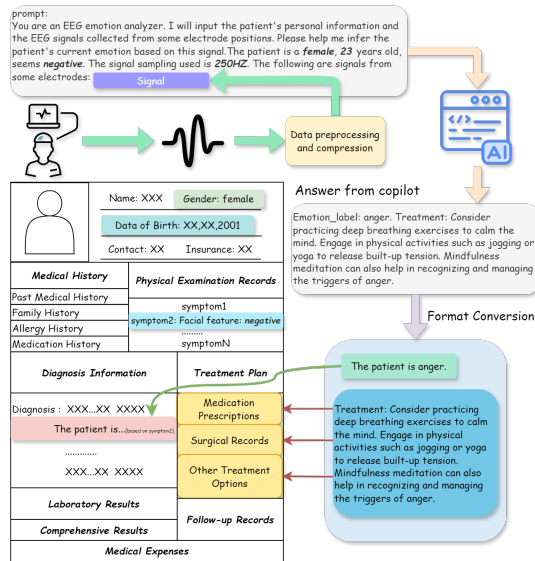


Fig. 12: An example using our EEG Emotion Copilot to create the assisted electronic medical record. Initially, the prompt is provided as the starting sentence, followed by the addition of the subject's demographic information, including gender, age, and certain facial features (female, 23 years old, negative). Finally, the preprocessed and compressed EEG signal is incorporated to complete the prompt, which is then input into EEG Emotion Copilot.

records. Our findings indicate that EEG Emotion Copilot has the potential to revolutionize the recognition and treatment of emotions in clinical settings, ultimately enhancing human-computer interaction and improving patient outcomes. Future work will combine lightweight LLMs with multimodal data such as human facial expressions, speech, gestures to achieve greater accuracy in affective computing.

## REFERENCES

- [1] R. W. Picard, *Affective computing*. MIT press, 2000.
- [2] X. Hu, J. Chen, F. Wang, and D. Zhang, "Ten challenges for eeg-based affective computing," *Brain sci. adv.*, vol. 5, no. 1, pp. 1–20, 2019.
- [3] Y. Wang, W. Song, W. Tao, A. Liotta, D. Yang, X. Li, S. Gao, Y. Sun, W. Ge, W. Zhang *et al.*, "A systematic review on affective computing: Emotion models, databases, and recent advances," *Inf. Fusion*, vol. 83, pp. 19–52, 2022.
- [4] M. Nardelli, G. Valenza, A. Greco, A. Lanata, and E. P. Scilingo, "Recognizing emotions induced by affective sounds through heart rate variability," *IEEE Trans. Affect. Comput.*, vol. 6, no. 4, pp. 385–394, 2015.
- [5] S. C. Leong, Y. M. Tang, C. H. Lai, and C. Lee, "Facial expression and body gesture emotion recognition: A systematic review on the use of visual data in affective computing," *Comput. Sci. Rev.*, vol. 48, p. 100545, 2023.
- [6] F. Eyben, K. R. Scherer, B. W. Schuller, J. Sundberg, E. André, C. Busso, L. Y. Devillers, J. Epps, P. Laukka, S. S. Narayanan *et al.*, "The geneva minimalistic acoustic parameter set (gemaps) for voice research and affective computing," *IEEE Trans. Affect. Comput.*, vol. 7, no. 2, pp. 190–202, 2015.
- [7] M. Pantic, N. Sebe, J. F. Cohn, and T. Huang, "Affective multimodal human-computer interaction," in *Proc. Int. Conf. on Multimedia*, 2005, pp. 669–676.
- [8] H. Altaheri, G. Muhammad, and M. Alsulaiman, "Physics-informed attention temporal convolutional network for eeg-based motor imagery classification," *IEEE Trans. Industr. Inform.*, vol. 19, no. 2, pp. 2249–2258, 2022.

- [9] J. J. Rivas, M. del Carmen Lara, L. Castrejon, J. Hernandez-Franco, F. Orihuela-Espina, L. Palafox, A. Williams, N. Bianchi-Berthouze, and L. E. Sucar, "Multi-label and multimodal classifier for affective states recognition in virtual rehabilitation," *IEEE Trans. Affect. Comput.*, vol. 13, no. 3, pp. 1183–1194, 2021.
- [10] S. U. Amin, H. Altaheri, G. Muhammad, W. Abdul, and M. Alsulaiman, "Attention-inception and long-short-term memory-based electroencephalography classification for motor imagery tasks in rehabilitation," *IEEE Trans. Industr. Inform.*, vol. 18, no. 8, pp. 5412–5421, 2021.
- [11] S. Greene, H. Thapliyal, and A. Caban-Holt, "A survey of affective computing for stress detection: Evaluating technologies in stress detection for better health," *IEEE Consum. Electr. M.*, vol. 5, no. 4, pp. 44–56, 2016.
- [12] S. M. Alarcao and M. J. Fonseca, "Emotions recognition using eeg signals: A survey," *IEEE Trans. Affect. Comput.*, vol. 10, no. 3, pp. 374–393, 2017.
- [13] J. Luo, W. Cui, S. Xu, L. Wang, X. Li, X. Liao, and Y. Li, "A dual-branch spatio-temporal-spectral transformer feature fusion network for eeg-based visual recognition," *IEEE Trans. Industr. Inform.*, vol. 20, no. 2, pp. 1721–1731, 2023.
- [14] M. Jafari, A. Shoebibi, M. Khodatars, S. Bagherzadeh, A. Shalbfaf, D. L. Garcia, J. M. Gorriz, and U. R. Acharya, "Emotion recognition in eeg signals using deep learning methods: A review," *Comput Biol. Med.*, p. 107450, 2023.
- [15] V. Padmashree and A. Bhattacharyya, "Human emotion recognition based on time–frequency analysis of multivariate eeg signal," *Knowl. Based Syst.*, vol. 238, p. 107867, 2022.
- [16] Y. Chang, X. Wang, J. Wang, Y. Wu, L. Yang, K. Zhu, H. Chen, X. Yi, C. Wang, Y. Wang *et al.*, "A survey on evaluation of large language models," *ACM Trans. Intell. Syst. Technol.*, vol. 15, no. 3, pp. 1–45, 2024.
- [17] A. J. Thirunavukarasu, D. S. J. Ting, K. Elangovan, L. Gutierrez, T. F. Tan, and D. S. W. Ting, "Large language models in medicine," *Nat. Med.*, vol. 29, no. 8, pp. 1930–1940, 2023.
- [18] A. Vaswani, "Attention is all you need," *Adv. Neural Inf. Process. Syst.*, 2017.
- [19] W. Talukdar and A. Biswas, "Improving large language model (llm) fidelity through context-aware grounding: A systematic approach to reliability and veracity," *arXiv preprint arXiv:2408.04023*, 2024.
- [20] J. W. Kim, A. Alaa, and D. Bernardo, "Eeg-gpt: exploring capabilities of large language models for eeg classification and interpretation," *arXiv preprint arXiv:2401.18006*, 2024.
- [21] Y. Zhang, Q. Li, S. Nahata, T. Jamal, S.-k. Cheng, G. Cauwenberghs, and T.-P. Jung, "Chatgpt-bci: Word-level neural state classification using gpt, eeg, and eye-tracking biomarkers in semantic inference reading comprehension," *CoRR*, 2023.
- [22] A. Yang, B. Yang, B. Hui, B. Zheng, B. Yu, C. Zhou, C. Li, C. Li, D. Liu, F. Huang *et al.*, "Qwen2 technical report," *arXiv preprint arXiv:2407.10671*, 2024.
- [23] E. J. Hu, Y. Shen, P. Wallis, Z. Allen-Zhu, Y. Li, S. Wang, L. Wang, and W. Chen, "Lora: Low-rank adaptation of large language models," *arXiv preprint arXiv:2106.09685*, 2021.
- [24] Y. Gao, Y. Xiong, X. Gao, K. Jia, J. Pan, Y. Bi, Y. Dai, J. Sun, and H. Wang, "Retrieval-augmented generation for large language models: A survey," *arXiv preprint arXiv:2312.10997*, 2023.
- [25] S. Merity, C. Xiong, J. Bradbury, and R. Socher, "Pointer sentinel mixture models," 2016.
- [26] C. Raffel, N. Shazeer, A. Roberts, K. Lee, S. Narang, M. Matena, Y. Zhou, W. Li, and P. J. Liu, "Exploring the limits of transfer learning with a unified text-to-text transformer," *arXiv e-prints*, 2019.
- [27] R.-N. Duan, J.-Y. Zhu, and B.-L. Lu, "Differential entropy feature for EEG-based emotion classification," in *Proc. 6th Int. IEEE/EMBS Conf. Neural Eng. (NER)*. IEEE, 2013, pp. 81–84.
- [28] J. Chen, X. Wang, C. Huang, X. Hu, X. Shen, and D. Zhang, "A large finer-grained affective computing eeg dataset," *Sci. Data.*, vol. 10, no. 1, p. 740, 2023.
- [29] V. Michel, L. Mazzola, M. Lemesle, and L. Vercueil, "Long-term eeg in adults: sleep-deprived eeg (sde), ambulatory eeg (amb-eeg) and long-term video-eeg recording (ltver)," *Neurophysiol. Clin.*, vol. 45, no. 1, pp. 47–64, 2015.
- [30] W.-L. Zheng and B.-L. Lu, "Investigating critical frequency bands and channels for eeg-based emotion recognition with deep neural networks," *IEEE Trans. Auton. Ment. Dev.*, vol. 7, no. 3, pp. 162–175, 2015.
- [31] I. Sturm, S. Lapuschkin, W. Samek, and K.-R. Müller, "Interpretable deep neural networks for single-trial eeg classification," *J. Neurosci. Methods.*, vol. 274, pp. 141–145, 2016.

- [32] S. Yasin, A. Othmani, I. Raza, and S. A. Hussain, "Machine learning based approaches for clinical and non-clinical depression recognition and depression relapse prediction using audiovisual and eeg modalities: A comprehensive review," *Comput. Biol. Med.*, vol. 159, p. 106741, 2023.
- [33] F. Hassan, S. F. Hussain, and S. M. Qaisar, "Fusion of multivariate eeg signals for schizophrenia detection using cnn and machine learning techniques," *Inf. Fusion*, vol. 92, pp. 466–478, 2023.
- [34] Y. Zhou, A. I. Muresanu, Z. Han, K. Paster, S. Pitis, H. Chan, and J. Ba, "Large language models are human-level prompt engineers," *arXiv preprint arXiv:2211.01910*, 2022.
- [35] A. Iyer, S. S. Das, R. Teotia, S. Maheshwari, and R. R. Sharma, "Cnn and lstm based ensemble learning for human emotion recognition using eeg recordings," *Multimed. Tools Appl.*, vol. 82, no. 4, pp. 4883–4896, 2023.
- [36] H.-I. Suk and S.-W. Lee, "A novel bayesian framework for discriminative feature extraction in brain-computer interfaces," *IEEE Trans. Pattern Anal. Mach. Intell.*, vol. 35, no. 2, pp. 286–299, 2012.
- [37] R. Li, J. S. Johansen, H. Ahmed, T. V. Ilyevsky, R. B. Wilbur, H. M. Bharadwaj, and J. M. Siskind, "The perils and pitfalls of block design for eeg classification experiments," *IEEE Trans. Pattern Anal. Mach. Intell.*, vol. 43, no. 1, pp. 316–333, 2020.
- [38] B. Wang, X. Fu, Y. Lan, L. Zhang, W. Zheng, and Y. Xiang, "Large transformers are better eeg learners," *arXiv preprint arXiv:2308.11654*, 2023.
- [39] P. Ramkumar, D. E. Acuna, M. Berniker, S. T. Grafton, R. S. Turner, and K. P. Kording, "Chunking as the result of an efficiency computation trade-off," *Nat. Commun.*, vol. 7, no. 1, p. 12176, 2016.
- [40] Z. Zheng, X. Ren, F. Xue, Y. Luo, X. Jiang, and Y. You, "Response length perception and sequence scheduling: An llm-empowered llm inference pipeline," *Adv. Neural Inf. Process. Syst.*, vol. 36, 2024.
- [41] X. Ma, X. Yang, W. Xiong, B. Chen, L. Yu, H. Zhang, J. May, L. Zettlemoyer, O. Levy, and C. Zhou, "Megalodon: Efficient llm pretraining and inference with unlimited context length," *arXiv preprint arXiv:2404.08801*, 2024.
- [42] J. Frankle and M. Carbin, "The lottery ticket hypothesis: Finding sparse, trainable neural networks," *arXiv preprint arXiv:1803.03635*, 2018.
- [43] Z. Liu, M. Sun, T. Zhou, G. Huang, and T. Darrell, "Rethinking the value of network pruning," *arXiv preprint arXiv:1810.05270*, 2018.
- [44] N. Jones, "Bigger ai chatbots more inclined to spew nonsense-and people don't always realize," *Nature*, 2024.
- [45] H. Li, A. Kadav, I. Durdanovic, H. Samet, and H. P. Graf, "Pruning filters for efficient convnets," *arXiv preprint arXiv:1608.08710*, 2016.
- [46] S. Han, H. Mao, and W. J. Dally, "Deep compression: Compressing deep neural networks with pruning, trained quantization and huffman coding," *arXiv preprint arXiv:1510.00149*, 2015.
- [47] P. Michel, O. Levy, and G. Neubig, "Are sixteen heads really better than one?" *Adv. Neural Inf. Process. Syst.*, vol. 32, 2019.
- [48] Z. Wang, J. Wohlwend, and T. Lei, "Structured pruning of large language models," *arXiv preprint arXiv:1910.04732*, 2019.
- [49] Z. Liu, H. Mu, X. Zhang, Z. Guo, X. Yang, K.-T. Cheng, and J. Sun, "Metapruning: Meta learning for automatic neural network channel pruning," in *Proc. IEEE Conf. Comput. Vis. Pattern Recog.*, 2019, pp. 3296–3305.
- [50] J. Guo, W. Zhang, W. Ouyang, and D. Xu, "Model compression using progressive channel pruning," *IEEE Trans. Circuits Syst. Video Technol.*, vol. 31, no. 3, pp. 1114–1124, 2020.
- [51] D. Blalock, J. J. Gonzalez Ortiz, J. Frankle, and J. Gutttag, "What is the state of neural network pruning?" *Proc. Int. Conf. Mach. Learn.*, vol. 2, pp. 129–146, 2020.
- [52] Y. He and L. Xiao, "Structured pruning for deep convolutional neural networks: A survey," *IEEE Trans. Pattern Anal. Mach. Intell.*, 2023.
- [53] E. Frantar and D. Alistarh, "Sparsegpt: Massive language models can be accurately pruned in one-shot," in *Proc. Int. Conf. Mach. Learn.* PMLR, 2023, pp. 10323–10337.
- [54] X. Ma, G. Fang, and X. Wang, "Llm-pruner: On the structural pruning of large language models," *Proc. Adv. Neural Inf. Process. Syst.*, vol. 36, pp. 21702–21720, 2023.
- [55] H. Touvron, T. Lavril, G. Izacard, X. Martinet, M.-A. Lachaux, T. Lacroix, B. Rozière, N. Goyal, E. Hambro, F. Azhar *et al.*, "Llama: Open and efficient foundation language models," *arXiv preprint arXiv:2302.13971*, 2023.
- [56] E. H. Shortliffe, "The evolution of electronic medical records," *Acad. Med.*, vol. 74, no. 4, pp. 414–9, 1999.
- [57] G. Fang, X. Ma, M. Song, M. B. Mi, and X. Wang, "Depgraph: Towards any structural pruning," in *Proc. IEEE Conf. Comput. Vis. Pattern Recog.*, 2023, pp. 16091–16101.
- [58] S. Zhang, S. Roller, N. Goyal, M. Artetxe, M. Chen, S. Chen, C. Dewan, M. Diab, X. Li, X. V. Lin, T. Mihaylov, M. Ott, S. Shleifer, K. Shuster, D. Simig, P. S. Koura, A. Sridhar, T. Wang, and L. Zettlemoyer, "Opt: Open pre-trained transformer language models," 2022.
- [59] Z. Cai, M. Cao, H. Chen, K. Chen, K. Chen, X. Chen, X. Chen, Z. Chen, Z. Chen, P. Chu, X. Dong, H. Duan, Q. Fan, Z. Fei, Y. Gao, J. Ge, C. Gu, Y. Gu, T. Gui, A. Guo, Q. Guo, C. He, Y. Hu, T. Huang, T. Jiang, P. Jiao, Z. Jin, Z. Lei, J. Li, J. Li, L. Li, S. Li, W. Li, Y. Li, H. Liu, J. Liu, J. Hong, K. Liu, K. Liu, X. Liu, C. Lv, H. Lv, K. Lv, L. Ma, R. Ma, Z. Ma, W. Ning, L. Ouyang, J. Qiu, Y. Qu, F. Shang, Y. Shao, D. Song, Z. Song, Z. Sui, P. Sun, Y. Sun, H. Tang, B. Wang, G. Wang, J. Wang, J. Wang, R. Wang, Y. Wang, Z. Wang, X. Wei, Q. Weng, F. Wu, Y. Xiong, C. Xu, R. Xu, H. Yan, Y. Yan, X. Yang, H. Ye, H. Ying, J. Yu, J. Yu, Y. Zang, C. Zhang, L. Zhang, P. Zhang, P. Zhang, R. Zhang, S. Zhang, S. Zhang, W. Zhang, W. Zhang, X. Zhang, X. Zhang, H. Zhao, Q. Zhao, X. Zhao, F. Zhou, Z. Zhou, J. Zhuo, Y. Zou, X. Qiu, Y. Qiao, and D. Lin, "Internlm2 technical report," 2024.
- [60] Qwen Team, "Qwen2.5: A party of foundation models," September 2024. [Online]. Available: <https://qwenlm.github.io/blog/qwen2.5/>
- [61] L. Van der Maaten and G. Hinton, "Visualizing data using t-sne." *J. Mach. Learn. Res.*, vol. 9, no. 11, 2008.
- [62] U. Von Luxburg, "A tutorial on spectral clustering," *Stat. Comput.*, vol. 17, pp. 395–416, 2007.
- [63] V. Viswanathan, K. Gashteovski, K. Gashteovski, C. Lawrence, T. Wu, and G. Neubig, "Large language models enable few-shot clustering," *Trans. Assoc. Comput. Linguist*, vol. 12, pp. 321–333, 2024.
- [64] H. Chen, W. Zeng, L. Cai, Y. Li, L. Wang, J. Lu, H. Yan, W. T. Siok, and N. Wang, "You only acquire sparse-channel (yoas): A unified framework for dense-channel eeg generation," *arXiv preprint arXiv:2406.15269*, 2024.
- [65] Y. Li, W. Zeng, W. Dong, D. Han, L. Chen, H. Chen, H. Yan, W. T. Siok, and N. Wang, "A tale of single-channel electroencephalogram: Devices, datasets, signal processing, applications, and future directions," *arXiv preprint arXiv:2407.14850*, 2024.
- [66] L. Zhou, W. Schellaert, F. Martínez-Plumed, Y. Moros-Daval, C. Ferri, and J. Hernández-Orallo, "Larger and more instructable language models become less reliable," *Nature*, pp. 1–8, 2024.